Response of concentrated suspensions under large amplitude oscillatory shear flow

Takatsune Narumi[a)]

Department of Mechanical and Production Engineering, Niigata University, 8050 2-no-cho Ikarashi, Niigata 950-2181, Japan

Howard See

Department of Chemical Engineering, The University of Sydney, NSW 2006, Sydney, Australia

Atsushi Suzuki and Tomiichi Hasegawa

Department of Mechanical and Production Engineering, Niigata University, 8050 2-no-cho Ikarashi, Niigata 950-2181, Japan

(Received 6 January 2004; final revision received 3 August 2004)

Synopsis

Concentrated suspensions of non-Brownian spheres dispersed in a Newtonian carrier liquid were placed under large amplitude oscillatory shear flow. It was found that the response wave forms consisted of a transient response after each reversal in the shearing direction, followed by purely viscous behavior. It was thought that rearrangements in the particulate microstructure could account for this transient response. Further, the characteristic strain for the microstructural rearrangement was found to be essentially independent of the oscillation frequency, and showed good agreement with the corresponding characteristic strain obtained from measurements of the transient response after shear reversal in continuous shear experiments. In addition, the fluidity in the oscillatory flow after the transient response was found to be higher than that in the steady flow case. This increase in fluidity was found to depend on the particle size dispersity, with the largest fluidity difference occurring with the monodispersed systems. © *2005 The Society of Rheology.*
[DOI: 10.1122/1.1814112]

I. INTRODUCTION

The rheology of suspensions is an important issue in many industrial processes. Examples include ceramic molding, food processing, production of cosmetics or composite materials, etc. Despite the fact that concentrated particulate suspensions occur in many industrial flow situations, we still only have a limited understanding of their fundamental rheological behavior. In this paper, we consider suspensions where the particles are at least several microns in size, allowing us to ignore the effects of Brownian motion. We focus on the specific problem of the response under large amplitude oscillatory shear flow of concentrated suspensions of spheres dispersed in a Newtonian carrier liquid. It will be

[a)]Author to whom all correspondence should be addressed; electronic mail: narumi@eng.niigata-u.ac.jp

seen that there are some parallels and differences between the behavior under large amplitude oscillatory flow and that under steady shear flow reported elsewhere (Narumi *et al.*, 2002).

Gadala-Maria and Acrivos (1980) have previously reported an experimental study of concentrated suspensions of 40–50 μm diameter polystyrene spheres in silicone oil under steady shear and oscillatory shear, where they focused on the transient stress responses and related these to the rearrangement of microstructure. Under the oscillatory deformations, they found that the suspensions exhibited nonsinusoidal wave forms, and that the shape of these curves could be predicted from the transient behavior observed in shear reversal experiments. Although in the latter tests they showed that these transient responses with constant shear rates ended after about 2 in strain, their oscillatory tests were conducted with strain amplitudes less than 2. Thus the responses after each reversal in direction in their oscillatory tests were affected by the incomplete microstructural rearrangement in the preceding cycle. There have also been other reports of particulate suspensions exhibiting nonsinusoidal wave forms under oscillatory shearing, such as Onogi *et al.* (1970), Matsumoto *et al.* (1973), and Doraiswamy *et al.* (1991), but these tests were conducted with very small oscillations and have focused on particles in viscoelastic carrier fluids. In these studies, the wave forms were analyzed by calculating the Fourier components, and the nonlinear behavior was attributed to the presence of a yield stress in the material. Recently, Heymann and co-workers (2002) examined the behavior of a suspension of poly(methylmethacrylate) (PMMA) spheres under oscillatory shear flow, with the main focus being on the onset of the nonlinear viscoelastic response as the stress amplitudes were increased. The nonlinearity was detected via a technique based on Fourier analysis of the resulting strain wave forms, with the appearance of higher harmonics (Wilhelm *et al.*, 1999). In the present paper, we will also deal with the case of a Newtonian carrier fluid, and we will explore the explanation for the transient response proposed by Gadala-Maria and Acrivos (1980), attributing it to the microstructural rearrangements after the periodic changes in shearing direction during the cyclical deformation. The Lissajous plot approach adopted in this study will be seen to provide many useful insights into the rearrangement process. For completeness, it should be pointed out that, in addition to rheometrical studies, there have also been experimental studies which monitor the microstructural development in suspensions via optical techniques (e.g., Voltz *et al.*, 2002) or observation of flow induced changes in particle concentrations (e.g., the study of bimodally sized systems by Hampton *et al.*, 1997).

On the theoretical side, there have recently been models developed which can predict some aspects of the experimentally observed strain-governed transient behavior after shear reversal. For example, Phan-Thien and co-workers have developed a constitutive model for concentrated suspensions of non-Brownian monodisperse spheres (Phan-Thien, 1995, Phan-Thien *et al.*, 1999, 2000), which is based on the motion of a generic pair of neighboring spheres in the suspension, with the interaction with surrounding spheres modeled by a diffusion-like process. As explained in our earlier paper (Narumi *et al.*, 2002), this model appears to be able to capture reasonably well the strain dependence of the transient response after shear reversal in steady shearing flows. However, this model predicts no dependence on the shear rate, and so would be unable to explain the significant dependence of the response on oscillation frequency, which has been observed under the large amplitude oscillatory shear flows to be presented in detail in this paper.

In this paper, we describe a series of oscillatory shear measurements we have carried out on suspensions of mono-, bi-, and polydispersed systems. We have mainly examined the effects of polydispersity in particle size and the frequency of the oscillations, thus extending the observations of Gadala-Maria and Acrivos (1980). Lissajous-type plots of

TABLE I. Mono- and polydispersed suspensions tested.

	MD5	MD10	PD6	PD10
Particle (trade name)	Benzo-guanamine melamine (GP-H50)	Benzo-guanamine melamine (GP-H100)	PMMA (MA-1006)	PMMA (MA-1010)
Average diameter[a]	4.96 μm	10.0 μm	6.97 μm	10.2 μm
S.D.[b]	0.20 μm	0.45 μm	2.53 μm	3.79 μm
Specific gravity	1.4	1.4	1.2	1.2
Carrier liquid	Silicone oil 1000cs (Specific gravity = 0.98)			
Volume fraction	$\phi = 0.5$			

[a]Volume base.
[b]Standard Deviation.

shear rate or strain against shear stress were used, and these enabled us to clearly see the postreversal transient behavior on the sinusoidal responses as well as facilitating comparison with results from steady shearing tests, via the power law viscous model. We found that the essential features of the response under oscillatory deformation agree with the description given by Gadala-Maria and Acrivos (1980). Some discrepancy was observed, however, between the steady and oscillatory responses particularly for the monodispersed systems.

This paper is organized as follows. In Sec. II we describe the materials and apparatus used. We show the experimental results and discuss these in Sec. III, comparing with our previous measurements performed under continuous shearing. Finally, in Sec. IV we present our concluding remarks.

II. EXPERIMENT

The particles used are summarized in Tables I and II. Basically, there were four kinds of spherical particles used, all manufactured by Nippon Shokubai Co. Ltd. (Japan): GP-H50 and GP-H100 of benzo-guanamine melamine spheres, and MA-1006 and MA-1010 of PMMA spheres. All particles were dispersed in silicone oil of viscosity 1.13 Pa s at 20 °C (manufactured by Shin-etsu Chemical Co., Ltd., Japan), at volume fraction of $\phi = 0.5$. The relevant material properties of the four basic particles are summarized in Table I. Since the GP-H particles have a very narrow size distribution, we have regarded the suspensions with these particles as monodispersed systems and will call these MD5 or MD10. The naming here is a combination of the label MD (for "monodispersed") with the average particle size in microns. The PMMA systems of PD6 and PD10 are considered as polydispersed (PD systems), with approximately same size range of diameter to

TABLE II. Bidispersed suspension tested.

(GP-H50:GP-H100)	BD5-10(3:1)	BD5-10(1:1)	BD5-10(1:3)
Volume ratio	3:1	1:1	1:3
Number ratio	24.8:1	8.26:1	2.74:1
Average diameter[a]	5.39 μm	6.02 μm	7.10 μm
Carrier liquid	Silicone oil 1000cs (specific gravity = 0.98)		
Volume fraction	$\phi_{total} = 0.5$		

[a]Volume base.

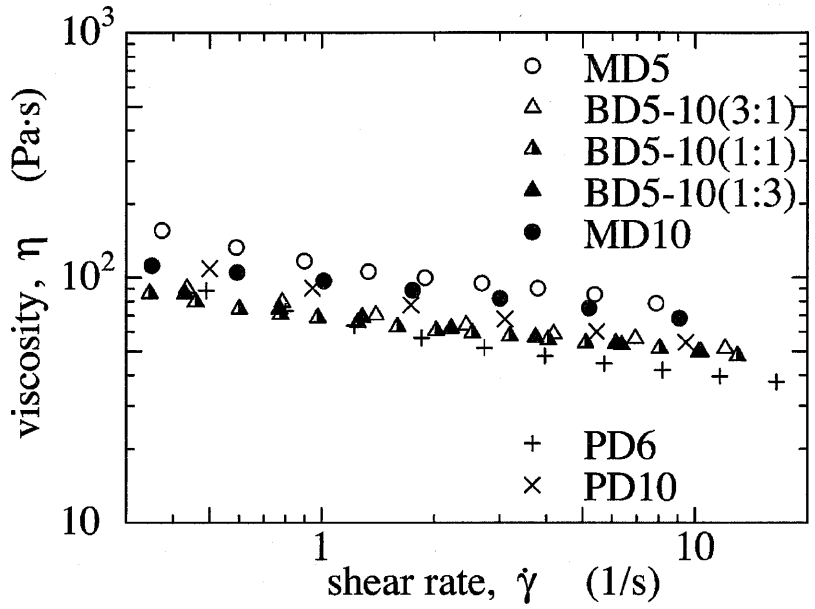

FIG. 1. Viscosity of test fluids measured in steady flow.

the monodispersed ones. In addition to these four basic particle types, we have tested three kinds of bidispersed suspensions as shown in Table II: blends of GP-H50 and GP-H100 ("BD" systems). Here, the small and large particles were mixed with volume ratio of 1:3, 1:1, or 3:1, and dispersed in the silicone oil with a total volume fraction of $\phi_{\text{total}} = 0.5$. Table II shows more details of the bidispersed systems. A synthetic resin and adhesive mixer (UM-102S, JAPAN UNIX) was used to ensure uniformity of the suspensions, and no significant clumping or sedimentation of the particles was observed after the suspension was made up. In particular, we have estimated the characteristic mean sedimentation time τ_s (the time required for a particle to sediment over its diameter) following the approach of Delhaye (2000) and Russel (1991), and this was found to be quite long ($\tau_s = 770$ min) even in the worst case. It should be pointed out that although there are different particulate materials used in this study, it will be assumed that all systems act essentially as hard-spheres.

Figure 1 illustrates the steady shear viscosities of the samples measured with a Haake stress-controlled rheometer (model RS-50) in the steady shearing mode. The tests were conducted with a cone-plate configuration with diameter 35 mm and cone angle of 2°. The minimum gap at the center was 112 μm and was larger than the typical particle size, since the largest particle included in our suspensions (i.e., in PD10) was about 25 μm in diameter. We see that all of the test fluids showed weak shear thinning characteristics.

The same rheometer and measurement geometry was used in the stress-controlled oscillatory shearing tests. For definiteness, the oscillatory shear tests were conducted at five frequencies: $f = 0.316$, 0.681, 1.00, 1.47, and 2.15 Hz. In this paper, we use the corresponding angular velocities to denote the conditions, i.e., $\omega = 1.99$, 4.28, 6.28, 9.24, and 13.5 (rad/s). The amplitude of the stress signal applied was varied from 200 to 1200 Pa. Since too high shear rates gave rise to flow instability at the outer edge in the oscillation tests, the maximum amplitude was adjusted depending on the frequency and the test fluid. The tests have consequently been conducted with maximum shear rate of 10–30 (1/s) and the induced strain amplitude was about 1–6, so the samples were indeed

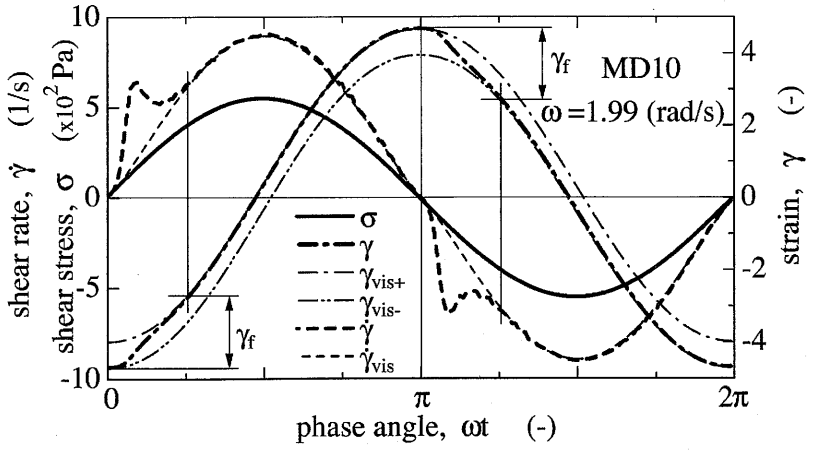

FIG. 2. Typical responses obtained for MD10 at $\omega = 1.99$ (rad/s) in oscillatory flow with sinusoidal stress applied of amplitude $\sigma_0 = 550$ (Pa). The resulting strain amplitude was $\gamma_0 = 4.68$.

subjected to large strains. The measurements of the oscillatory response were commenced after several cycles had been completed, as preset by the control system of rheometer. We will discuss the reproducibility of the response in the next section. The resulting strain waveforms were monitored using an oscilloscope connected to the rheometer. All tests were performed at 20±0.5 °C.

In these conditions, the Reynolds number for the particle-carrier liquid system (based on the difference in densities, particle diameter, velocity of the upper rheometer surface, and carrier liquid viscosity) is less than 0.01, so that we can consider inertial effects to be negligible. It should also be pointed out that several measurements were carried out for over an hour, and over this period no significant change in the response curves was observed. This supports the notion that sedimentation and particle migration were not significantly occurring in these systems. Further, visual inspection of the samples at the conclusion of each test did not reveal any major nonuniformities in the distribution of the particulates.

III. RESULTS AND DISCUSSION

A. Key features of the response

Figure 2 shows typical wave forms obtained for the MD10 sample at $\omega = 1.99$ (rad/s). Applying a sinusoidal stress (σ), a quarter-cycle ($\pi/2$) shifted and somewhat distorted sinusoidal strain response (γ) is obtained. The shear rate ($\dot{\gamma}$) estimated from the strain is also shown in Fig. 2. We see significant transient deviation in shear rate after the change in the shearing direction (at $\omega t = 0, \pi$). To clarify these features, the response wave forms were plotted in Fig. 3 in a Lissajous fashion as shear stress versus shear rate and strain. The arrows in Fig. 3 indicate the direction of the deformation during the cycles. The transient responses in shear rate after the reversals appear as a butterfly-shaped pair of curves in the upper part of Fig. 3. Similar figures were obtained for all samples tested (we will not show all plots here for conciseness). For any particular sample and measurement condition, it was confirmed that the curves were highly reproducible. Indeed it was observed that the form of the curve was essentially established after the first cycle had been applied—this also means that the samples were not sensitive to the prehistory of the sample before each test, provided that some agitation had occurred beforehand to

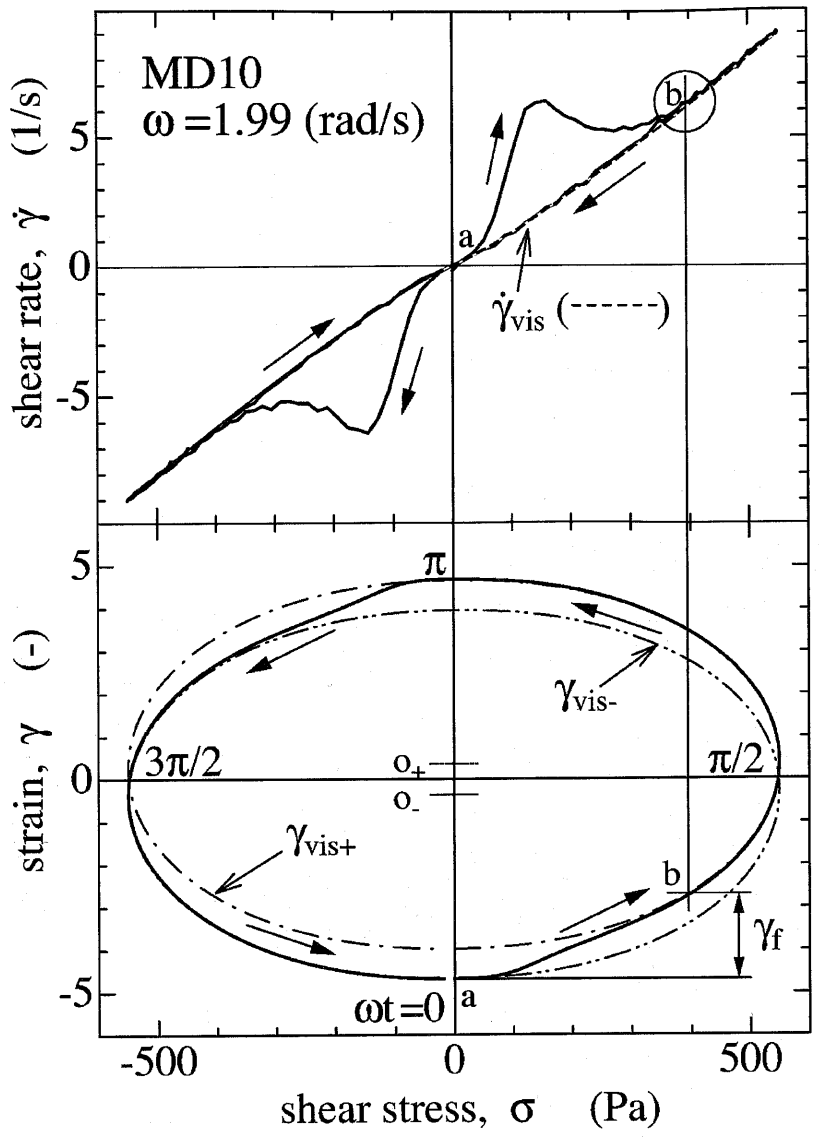

FIG. 3. Lissajous-type plots of shear rate (upper) or strain (lower) against shear stress for the same data in Fig. 2.

ensure good dispersion. As Fig. 2 shows, it was found for all suspensions that the rheological response was close to a liquid-like behavior with no solid-type response. That is, during each cycle, when the applied shear stress passed through zero, the strain was at a maximum or minimum value and the shear rate was zero (no phase lag).

The next step taken was to use a rheological model to fit the wave forms. We sought a simple model which captures the above behavior, in particular the fact that the shear stress and shear rate simultaneously pass through zero during each cycle. The curve $\dot{\gamma}_{vis}$ in Figs. 2 and 3 is such a purely viscous response estimated with the following power law model:

$$\sigma = m|\dot{\gamma}|^{n-1} \cdot \dot{\gamma}, \tag{1}$$

where $m = 81.1\,\mathrm{Pa\,s}^n$ and $n = 0.873$ in this case (MD10 sample). We see that $\dot{\gamma}_{vis}$ is in good agreement with the experimental one except for the transient periods. Two corresponding strain curves of γ_{vis+} and γ_{vis-} were also evaluated from integration of $\dot{\gamma}_{vis}$ with different initial conditions and these have been plotted in Figs. 2 and 3. We see from Fig. 2 that the strain curve (γ) obtained in the oscillatory flow with large deformation alternately fits on the two purely viscous responses of γ_{vis+} and γ_{vis-} via transient regions. In Fig. 3, γ_{vis+} and γ_{vis-} make two "viscous ellipses" with the same shape and the strain is alternately shifted from one to the other with transient periods. This means that the center of oscillation in strain is shifted (e.g., o_- to o_+ in Fig. 3) by the transient behavior after the shear reversal in these controlled stress tests.

Thus, it is clear that the wave forms of strain in Figs. 2 and 3 (lower part) show a gradual departure just after a change in the shearing direction, with the strain curve eventually shifting to the other viscous ellipse. Since the amplitudes of the strain induced in our oscillatory tests were large enough, this shift ended within a quarter cycle of deformation. Hence, we could easily estimate the transient period from the oscillatory data, that is, a characteristic strain γ_f. The following procedure was adopted: We found that γ_f could be neatly obtained if we focus on the curves in the stress-shear rate plots which join up with the power law curve before a quarter cycle of the deformation has been completed (i.e., we can see in the top right corner of Fig. 3 that this curve meets the power law line before the maximum shear stress has been applied). That is, for this curve we can define a merging point "b" as in Fig. 3, and γ_f can then be obtained as the corresponding strain from the reversal point "a" to b on the strain curve in the lower part of Fig. 3. From Fig. 3, we see that once a point like b has been passed, the curves follow the viscous ellipse as discussed previously, and that they then continue to follow the power law behavior as the applied stress is reduced back to zero.

We now consider the influence of the stress amplitude applied. Figure 4 shows representative sets of Lissajous plots of shear rate against shear stress obtained with the BD5-10(1:3) sample at an angular velocity of 4.28 (rad/s). Four curves with different stress amplitudes are respectively illustrated in the figure and we observe the similar butterfly-shaped curves which extended further from the center of the figure as the amplitude was increased. We see that the purely viscous responses after the transient ones trace the same line, regardless of the stress amplitude applied. Hence, we can define "power-law model"-based curves for respective frequencies similar to the $\dot{\gamma}_{vis}$ in Fig. 3. The model curve thus obtained is shown with a thickened line in Fig. 4. Moreover, the axes of shear stress and shear rate adopted here enable the stress values under steady shearing to also be readily plotted, facilitating comparison between the oscillatory and continuous shearing modes. Thus, the plot of steady viscosity (from Fig. 1) has also been presented in Fig. 4.

We now further explore the transient response after the reversal in flow direction. In order to clarify the transient response observed in the butterfly-shaped curves, we define an apparent viscosity (η_{ap}) defined by $\eta_{ap} = \sigma/\dot{\gamma}$. Still focusing on the BD5-10(1:3) sample, Fig. 5 illustrates the typical change in apparent viscosity with the shear strain after the reversal, where in this figure $\gamma = 0$ corresponds to the point a in Fig. 3. Three data sets with different stress amplitudes have been plotted for the three frequency conditions. It is interesting to observe that the apparent viscosity response shows good data collapse for each angular velocity with little dependence on the stress amplitude, similar to the behavior seen in Fig. 4 (previous paragraph). There is a clear reduction in η_{ap} just after the reversal, followed by a gradual increase to the quasi steady state values. This behavior parallels that seen in previous experiments involving continuous shearing, whereby the shear stress showed a gradual transient response after a sudden reversal of

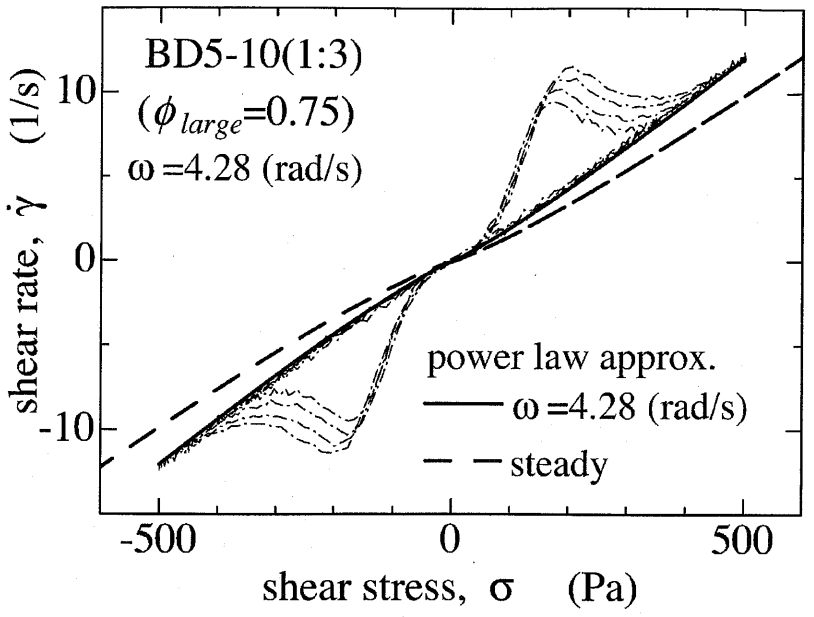

FIG. 4. Representative sets of Lissajous plots of shear rate against shear stress obtained with BD5-10(1:3), all obtained at the same frequency of ω = 4.28 (rad/s). The corresponding pairs of strain and stress amplitudes γ_0 / σ_0 (Pa) were: 2.23 / 350 (Pa), 2.51 / 400 (Pa), 2.83 / 450 (Pa), 3.10 / 500 (Pa). A power law approximation estimated after transient responses (thick line) is also compared with the prediction from the steady viscosity in Fig. 1 (thick broken line).

shearing direction (Narumi *et al.*, 2002). In these continuous deformation tests, the system was observed to eventually reach the steady state stress value after a typical strain (approximately 2), and it was considered that this response was related to the development of a microstructure of the particulates. Indeed, the magnitude of the strain (approximately 2) is similar to the critical strain amplitudes observed in this study (e.g., Fig. 5), and to the results of Gadala-Maria and Acrivos (1980) who used a concentric cylinder system.

Thus, similar to the steady shearing case, in the oscillatory flow case reported here, we believe that some kind of particulate microstructure generated in the previous half cycle is being broken up by the reversal and then being rearranged to reach a quasisteady state during the subsequent flow. The question arises as to the nature of the structures which may be developing in these systems. Since there appeared to be no yield stress or solid-like behavior observed in our tests for all samples, we think that it is reasonable to imagine a weakly aggregated, partially clumped structure being generated as the particulate undergoes flow in one direction. Moreover, during this transient process, the state with the highest fluidity, that is, with the minimum apparent viscosity $(\eta_{ap})_{min}$ (corresponding to the dip shown in Fig. 5), would be expected to be close to a state with almost no microstructure: that is, the reversal of direction has destroyed the previous structure, and the new structure is still being developed at this point in the cycle.

The preceding discussion has shown that flow characteristics in both the quasisteady state and the transient period display many common features, but that there is a clear dependence on the angular velocity. In the next subsection, we will consider the influence of particle size dispersion on the flow characteristics, with a particular focus on the angular velocity dependence.

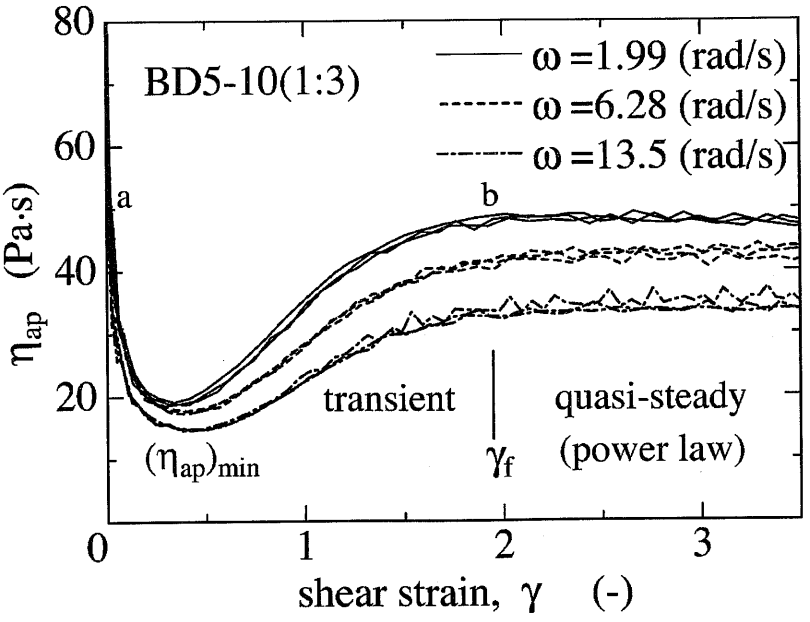

FIG. 5. Typical apparent viscosity $\eta_{ap} = \tau/\dot{\gamma}$ changes after shear reversal. Three data sets (each with different stress and strain amplitudes) are plotted for three frequency conditions. The respective pairs of γ_0/σ_0 (Pa) are 2.86 / 250 (Pa), 3.93 / 350 (Pa), 4.49 / 400 (Pa) for the frequency ω = 1.99 (rad/s), 2.47 / 600 (Pa), 2.68 / 650 (Pa), 2.92 / 700 (Pa) for the frequency ω = 6.28 (rad/s), and 1.97 / 800 (Pa), 2.25 / 900 (Pa), 2.48 / 1000 (Pa) for the frequency ω = 13.5 (rad/s). Observe that the strain from the reversal to the next one, i.e., twice the strain amplitude, would be larger than about 4 for all cases. The critical strain, γ_f, has been indicated on the figure to facilitate discussion.

B. Angular velocity dependence and particle size effects

The previous subsection focussed on two samples, MD10 and BD5-10(1:3), in order to present the key features of the response observed in these systems under oscillatory shear flow. We now expand the discussion to consider the range of polydisperse and bidisperse systems studied in this work, as listed in Tables I and II.

We first consider the response of the mono- and bimodal systems (MD and BD). The constants in the power model [Eq. (1)] were determined in the quasisteady states, as before. Figure 6 shows the power law index n for these systems plotted against the fraction of large particles ($\phi_{large}/\phi_{total}$), where 0 and 1 of the abscissa respectively indicate the monodisperse MD5 and MD10. Note that although a somewhat smaller n was obtained with the steady flow tests, there is not a large difference from the oscillatory results. Hence, we conclude that the power law index n has little dependence on frequency ω or the degree of particle size dispersity in these bimodal suspensions. On the other hand, Fig. 7 shows that the parameter m, which is equivalent to the viscosity at $\dot{\gamma}$ = 1 (1/s), has some dependence on both the frequency and the particle size dispersity. It is pointed out that the value of $m[= \eta(\dot{\gamma} = 1)]$ for the steady flow case followed a well-known trend with a dip occurring at an intermediate mixing for bimodal suspensions (e.g., Farris, 1968, D'Haene and Mewis, 1994). We observe that for the oscillatory tests, the value of m was significantly reduced, compared to the steady state case: this reduction in viscosity (= high fluidity) was particularly apparent with the monodisperse MD systems at the higher frequencies. The physical reason for the frequency dependence of this behavior is unclear—this will be the object of more detailed future studies.

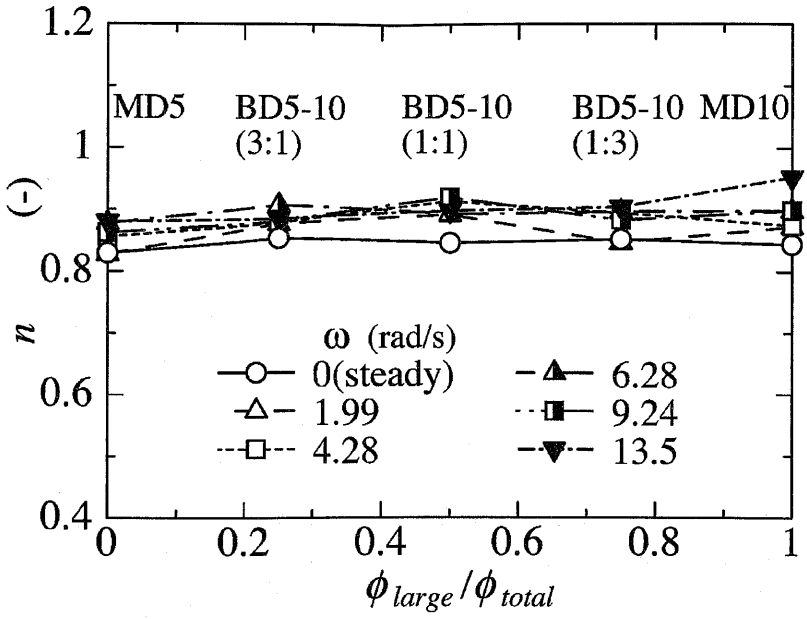

FIG. 6. Power law index n against the fraction of large particle for mono- and bidispersed systems.

Figure 7 also shows the variation of $(\eta_{ap})_{min}$, the minimum apparent viscosity obtained in the transient responses (i.e., the "dip" in Fig. 5). We see that there is almost no dependence of $(\eta_{ap})_{min}$ on the frequency or the size dispersity.

The earlier features observed in Fig. 7 suggest that the following may be a possible picture of the microstructural mechanisms governing these suspensions under large amplitude oscillatory shear flow. In the transient period immediately after the shear reversal, the microstructure of the particles would begin to be broken up. As the flow continues in

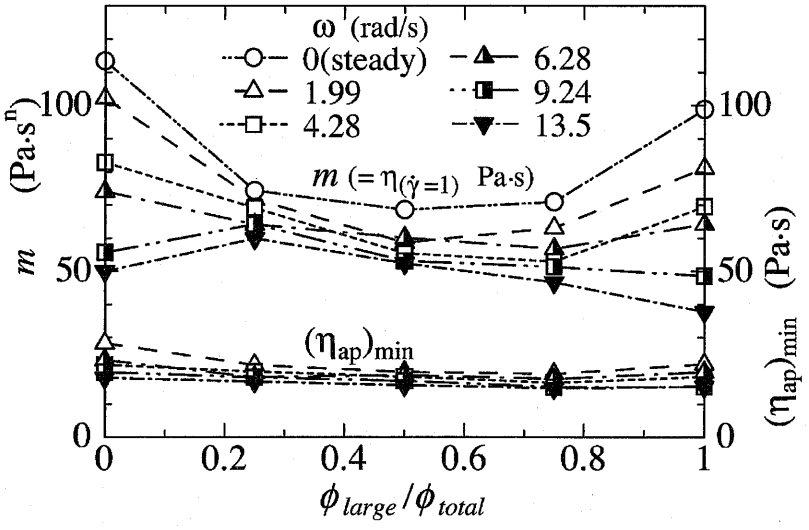

FIG. 7. Power law model parameter m, which is equivalent to the viscosity at $\dot{\gamma} = 1$ (1/s), for mono- and bidispersed systems.

the new direction, a common feature of all the particulate systems was that they passed through a state with minimum apparent viscosity [$(\eta_{ap})_{min}$ in Fig. 5]. This state is expected to correspond to one where the particles are not arranged in a structured way at all, and we observe from Fig. 7 that there was almost no difference in $(\eta_{ap})_{min}$ due to the frequency or the size dispersity. This suggests that the state corresponding to $(\eta_{ap})_{min}$ may serve as a useful basis state, upon which we can compare and monitor the subsequent changes in the microstructure and viscosity.

As the flow continues to be applied after the reversal, the particles begin to be arranged into their quasisteady state structures. These microstructures may possibly consist of aggregates of weakly bound particles, as mentioned previously. The dependence of m on the frequency (as seen in Fig. 7) could thus be attributed to the fact that the size of the aggregates formed in these stages of the oscillatory flow would depend on the angular velocity applied. Further, at lower frequencies, the MD systems in particular would be expected to produce more regularly ordered and larger aggregates because of their particle size monodispersity, thus leading to a larger viscosity (as seen in Fig. 7). Admittedly, this discussion of the microstructure and its changes during oscillatory flow is necessarily speculative since we do not have any direct microscopic information. Nevertheless, it would appear that much of the behavior can be interpreted in terms of microstructural ideas such as these.

The earlier discussion has focused on the mono- and bidisperse cases (MD and BD). Summarizing the key points so far, it can be said that the concentrated suspensions displayed not only shear thinning behavior of the viscosity for a certain frequency (i.e., the power law behavior seen under a fixed frequency in Fig. 4), but, in addition, a type of "dynamic shear thinning" behavior of the parameter m in oscillatory flow—that is, $m = m(\omega)$ which decreased with ω. Moreover, it was observed that this dynamic thinning of m strongly depended on particle size dispersity. Other interesting features which can be seen in Fig. 7 are that, as the frequencies become higher, the values of m are close for the two monodisperse systems, and furthermore that m appears to become less sensitive to ω and to the size composition.

We now turn to the flow characteristics of the polydispersed systems in the oscillatory tests. PD6 and PD10 have nearly the same shear thinning properties as those of other samples shown in Fig. 6; that is, PD6 has $n = 0.78-0.91$ and PD10 has $n = 0.79-0.87$. Figure 8 illustrates the power law constant m and the minimum apparent viscosity $(\eta_{ap})_{min}$ against the angular velocity for the polydispersed systems. The data of MD5 and BD5-10(1:1) are also plotted in Fig. 8 for comparison. We see that the PD systems show a similar trend to the bimodal ones with regards to the reduction of the parameter m with the oscillation frequency. Since the particles in both the PD systems have the normal distribution in size (not shown here), it is considered that PD6 and PD10 may show behavior close to the BD5-10(1:1) suspension. Indeed, since the $(\eta_{ap})_{min}$ values of the PD systems are similar to those of the other systems and are independent of the angular velocity, it is reasonable to expect that similar considerations to the bimodal case regarding the microstructure of the suspensions would be applicable to these polydispersed systems.

C. Characteristic strain γ_f in transient response

In this subsection, we will be concerned with the characteristic strain γ_f for the transient response as obtained in Figs. 3 and 5. Since the evaluation method of γ_f mentioned in the discussion of Figs. 3 and 4 (Sec. III A) is only applicable for cases where strain in the quarter cycle is larger than about 2, we determined γ_f only in the tests

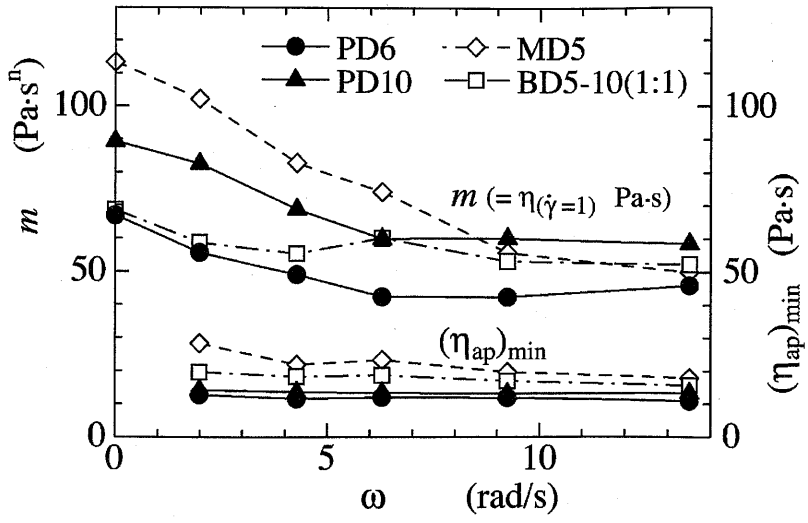

FIG. 8. Power law model parameter m, which is equivalent to the viscosity at $\dot{\gamma} = 1$ (1/s), for polydispersed systems.

where $\gamma_0 > 2.5$. Figure 9 shows the values for γ_f obtained with the mono- and bidispersed suspensions. There seems to be a slight dependence of γ_f on the fraction of large particles ($\phi_{\text{large}}/\phi_{\text{total}}$). However, it should be kept in mind that γ_f includes an error of about 20% in our digital estimation, so that we cannot definitely conclude that there is a significant dependence of γ_f on the frequency or the size dispersity, etc. Figure 10 shows that similar features and nearly the same values of γ_f are observed for the polydispersed systems. However, it is interesting to observe that the same γ_f was obtained for the

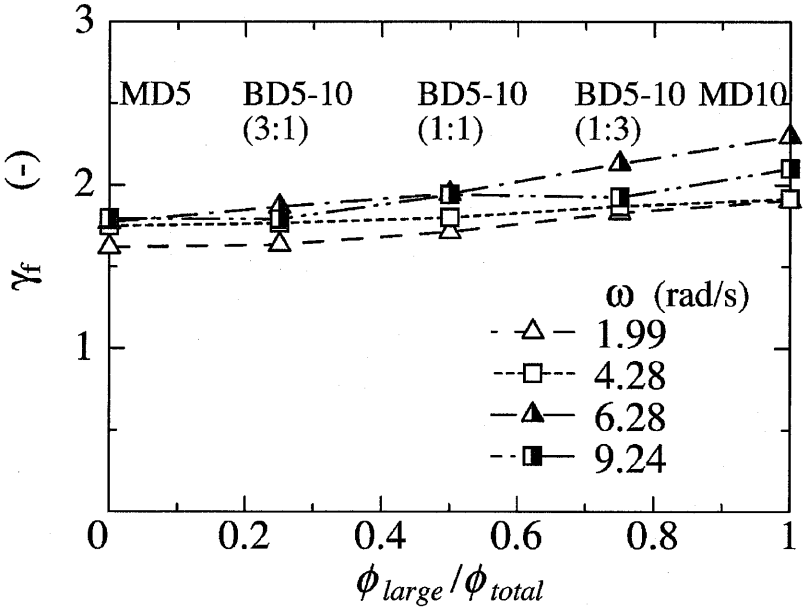

FIG. 9. Characteristic strain γ_f for the microstructural rearrangement estimated with the transient response after the shear reversal in oscillatory flow of mono- and bidispersed systems.

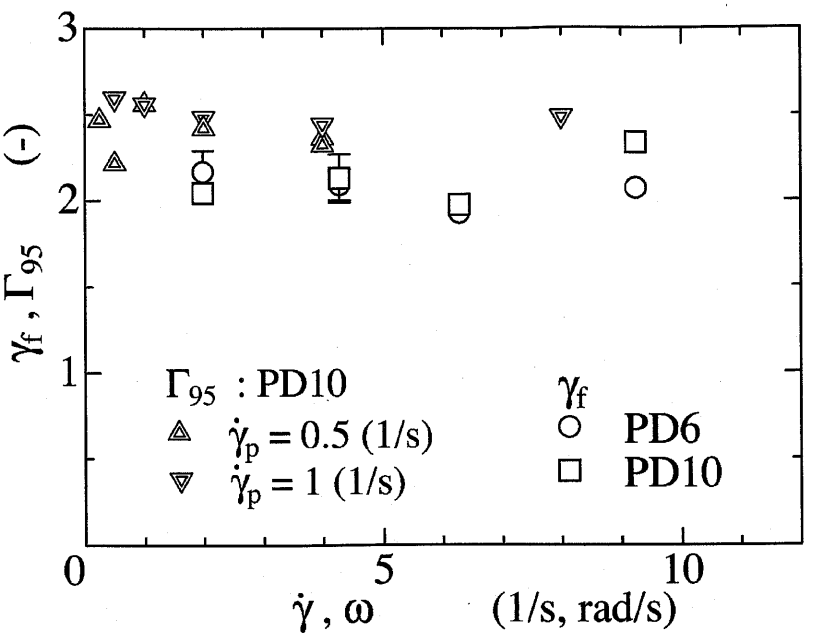

FIG. 10. Characteristic strain γ_f for the microstructural rearrangement in oscillatory flow of polydispersed system and corresponding characteristic strain Γ_{95} obtained from measurements of the transient response after shear reversal in continuous shear tests conducted.

different frequencies, whereas, as discussed in the previous subsections, the nature of the microstructures at the quasisteady states appear to have a distinct frequency dependence (Figs. 5 and 7). The characteristic strain, Γ_{95}, previously measured in the continuous deformation tests on the PD10 suspension, is also plotted in Fig. 10 for comparison (Narumi *et al.*, 2000, 2002). In those tests with a parallel plates system, Γ_{95} was defined as follows: it is the strain required for 95% of the steady shear stress to be recovered after the sudden reversal in the shearing direction. Figure 10 shows that there is reasonable agreement between γ_f and Γ_{95}. This tends to support the essential physical picture originally proposed by Gadala-Maria and Acrivos (1980) and which we have been adopting in this paper, whereby the departure from the simple viscous response in the oscillatory tests reflects the change in microstructure as the system recovers from each reversal in shearing direction. This behavior parallels that seen in the continuous shear tests. The independence of γ_f from the flow conditions (as seen in Figs. 9 and 10) also supports the argument that strain-governed microstructural rearrangement may be behind this phenomenon. Our data indicate that a strain of about 2 is necessary to rearrange the microstructure after the reversal. Thus, if the strain amplitude is not so large [as was the case in the tests of Gadala-Maria and Acrivos (1980)], the rearrangement process after the reversal would be affected by the shear history in the preceding half-cycle. On the other hand, the study by Heymann and co-workers (2002) on the onset of the nonlinear viscoelastic response in oscillatory shear tests is expected to be related to the characteristic strain in our study, since, in their constant frequency tests, they observed the strain amplitude decreasing as the stress amplitudes were decreased.

IV. CONCLUSIONS

We have carried out a series of large amplitude oscillatory shear measurements on concentrated suspensions of non-Brownian spheres dispersed in a Newtonian carrier liquid. It was found that the response wave forms consisted of the transient region after the shear reversal, followed by a purely viscous response which could be fitted by a power law-type model. It was thought that rearrangements in the particulate microstructure could account for the transient response after the shear reversal in each deformation half-cycle. In particular, it was observed that there was a clear reduction in the apparent viscosity just after the reversal, followed by a gradual increase to a "quasisteady state" value, indicating changes in the particle configurations. For a fixed angular velocity of the oscillation, it was found that the strain dependence of this apparent viscosity response showed good data collapse, with little dependence on the amplitude of the stress applied. Moreover, it was found that the minimum viscosity value and the characteristic strain in these transient responses showed little dependence on the angular velocity or the nature of the size dispersity of the particles. We also found that the values of the pseudoplastic viscosity m, estimated in the quasisteady states, was significantly reduced, compared to those obtained in the steady state tests: this reduction in viscosity was particularly apparent with the monodisperse systems at the higher frequencies.

Concentrated suspensions are a very important class of materials in industry, and an understanding of their flow behavior is essential for optimizing their processability and function. The results of this work lend further support to the basic concept of strain-driven microstructural change being the main governing process in the transient behavior observed in these systems.

ACKNOWLEDGMENT

The authors gratefully acknowledge the help of Yasuhiro Okada in the experimental stages of this project.

References

D'Haene, P., and J. Mewis, "Rheological characterization of bimodal colloidal dispersions," Rheol. Acta **33**, 165–174 (1994).

Delhaye, N., A. Poitou, and M. Chaouche, "Squeeze flow of highly concentrated suspensions of spheres," J. Non-Newtonian Fluid Mech. **94**, 67–74 (2000).

Doraiswamy, D., A. N. Mujumdar, I. Tsao, A. N. Bersi, S. C. Danforth, and A. B. Metzner, "The Cox–Merz rule extended: A rheological model for concentrated suspensions and other materials with a yield stress," J. Rheol. **35**, 647–685 (1991).

Farris, R. J., "Prediction of the viscosity of multimodal suspensions from unimodal viscosity data," Trans. Soc. Rheol. **12**, 281–301 (1968).

Gadala-Maria, F., and A. Acrivos, "Shear-induced structure in a concentrated suspension of solid spheres," J. Rheol. **24**, 799–814 (1980).

Hampton, R. E., A. A. Mammoli, A. L. Graham, N. Tetlow, and S. A. Altobelli, "Migration of particles undergoing pressure-driven flow in a circular conduit," J. Rheol. **41**, 621–640 (1997).

Heymann, L., S. Peukert, and N. Aksel, "Investigation of the solid-liquid transition of highly concentrated suspensions in oscillatory amplitude sweeps," J. Rheol. **46**, 93–112 (2002).

Matsumoto, T., Y. Segawa, Y. Warashina, and S. Onogi, "Nonlinear behavior of viscoelastic materials. II. The method of analysis and temperature dependence of nonlinear viscoelastic functions," Trans. Soc. Rheol. **17**, 47–62 (1973).

Narumi, T., Y. Honma, T. Hasegawa, T. Takahashi, H. See, and N. Phan-Thien, "Transient behavior of concentrated suspensions after a stepwise change in shear direction," Proc. XIIIth International Congress on Rheology, Cambridge UK, 2000, Vol. 4, pp. 193–195.

Narumi, T., H. See, Y. Honma, T. Takahashi, T. Hasegawa, and N. Phan-Thien, "Transient response of concentrated suspensions after shear reversal," J. Rheol. **46**, 295–305 (2002).

Onogi, S., T. Masuda, and T. Matsumoto, "Non-linear behavior of viscoelastic materials. I. Disperse systems of polystyrene solution and carbon black," Trans. Soc. Rheol. **14**, 275–294 (1970).

Phan-Thien, N., "Constitutive equation for concentrated suspensions in Newtonian liquids," J. Rheol. **39**, 679–695 (1995).

Phan-Thien, N., X. J. Fan, and B. C. Khoo, "A new constitutive model for monodispersed suspensions of spheres at high concentrations," Rheol. Acta **38**, 297–304 (1999).

Phan-Thien, N., X. J. Fan, and R. Zheng, "A numerical simulation of suspension flow using a constitutive model based on anisotropic interparticle interactions," Rheol. Acta **39**, 122–130 (2000).

Russel, W. B., D. A. Saville, and W. R. Schowalter, *Colloidal Dispersions* (Cambridge University Press, Cambridge, 1991), pp. 394–426.

Voltz, C., M. Nitschke, L. Heymann, and I. Rehberg, "Thixotropy in macroscopic suspensions of spheres," Phys. Rev. E **65**, 051402 (2002).

Wilhelm, M., P. Reinheimer, and M. Ortseifer, "High sensitivity Fourier-transform rheology," Rheol. Acta **38**, 349–356 (1999).